Mass Spectrometric Analysis of a Thermal Plasma Used for CVD of Diamond Films

Peter G. Greuel, Jeffrey T. Roberts and Douglas W. Ernie

University of Minnesota, Departments of Chemistry and Electrical Engineering, Minneapolis, MN 55455

Abstract

An apparatus has been constructed for mass spectrometric analysis of the gas phase composition in the growth region of a high-pressure, high-power thermal plasma used for the deposition of diamond films. Growth precursor and other gaseous species present near the substrate surface are extracted through a supersonic nozzle into a mass spectrometer. Threshold ionization mass spectrometry with pulse counting is used for detection of CH_x ($x \leq 3$) radical species. Measurements of the stable species CH_4, C_2H_2, C_2H_4 and C_2H_6, and of CH_x radicals as a function of discharge parameters and film quality/morphology are in progress. Preliminary results indicate the most abundant C_2 species is C_2H_2, followed by C_2H_4, with little detectable C_2H_6. In addition, the concentration of methyl radical (CH_3) during deposition has been found to be 2 PPM ± 20%.

Introduction

The economic potential of an efficient plasma-assisted diamond fabrication process at or near atmospheric pressure has led to a great deal of research. Several mechanisms for diamond growth have been proposed [1-3]. Typically these mechanisms are based on computer simulations that incorporate known gas phase reaction rates and unknown surface reaction rates, which are inferred from the analogous gas phase chemistry, to determine species concentration profiles in the growth region of the films. A direct quantitative measure of all species present at a growing diamond surface would be of use in verifying the simulations and elucidating the growth mechanism.

Experimental determination of the gas phase composition in the boundary layer above the growing film is not trivial. Standard spectroscopic techniques such as optical emission, laser induced fluorescence and infrared absorption have been used to detect partial gas phase composition during diamond deposition [4-6]. While non-intrusive, these techniques are only applicable to a limited number of species. Gas chromatography (GC) can be used to monitor a larger number of species and is currently being applied to the composition of atmospheric diamond growth in a rf

thermal plasma-assisted system similar to the apparatus described herein [7]. However, concentrations of reactive species such as methyl radicals cannot be directly measured with a conventional GC because they chemically react before reaching the detector.

A number of researchers have used mass spectrometry in thermal plasma-assisted CVD by introducing a sampling port adjacent to the diamond growth region [8-10]. In these systems, the mean free path for species entering the extraction port is small compared to the distance they traverse before detection. For reactive species, such as radicals, this is problematic since they may chemically react upon collision with other species. Hsu *et al.* and Sugai *et al.* have used molecular beam mass spectrometry coupled with threshold ionization techniques to measure reactive species concentrations near a growing diamond surface in low pressure, non-thermal rf plasma CVD reactors [11,12]. The design discussed herein is similar to these systems except that it is applied to a much higher pressure and temperature source.

Design

The apparatus, schematically depicted in Fig 1, has been designed for the detection of species that impinge on a substrate surface during rf thermal plasma-assisted diamond CVD. A rf induction plasma was chosen as the activation source to avoid contamination from electrode or filament vaporization. The detection scheme employs a quadrupole mass spectrometer (QMS) in conjunction with a supersonic sampling orifice to facilitate the detection of radical and stable species present near the substrate surface during diamond growth. The system is best described by breaking it down into three sections (labeled A, B and C in Fig. 1), with each lettered section corresponding to a different pressure region within the system.

The feedstock gases are dissociated and activated in the reactor (A), which consists of two concentric cylindrical quartz tubes mounted on a 14″ SS support plate with pumping ports. Water flows between the tubes to provide cooling. A 15 kW, 3.3 MHz rf power supply is coupled to the plasma volume via a five turn copper induction coil wrapped helically around the center of the outer quartz tube. Argon is injected through 36 uniformly spaced sheath ports that reside at a 45° angle tangent to the inside quartz cylinder. The reactant gases hydrogen and methane, along with Ar carrier gas, are fed into the system through an injection probe located centrally within the reactor volume. The height of the injection probe can be adjusted to control where the reactant gases enter the plasma. While the pressure in the reactor (P_1) can be varied from 760 to 1 torr by adjusting the pumping speed and/or the gas feed rate, QMS operation requires that the upstream pressure in the reactor be ≤ 400 torr. Typical discharge conditions are: plate power, 11 kW; reactor pressure, 200 torr; and $Ar/H_2/CH_4$ ratio, 11/1/0.015. Gaseous species activated in the plasma impinge on the substrate surface, where diamond growth occurs. The growth species are extracted through a small, cylindrical channel in the center of the molybdenum substrate and expanded through a supersonic nozzle into the differential stage.

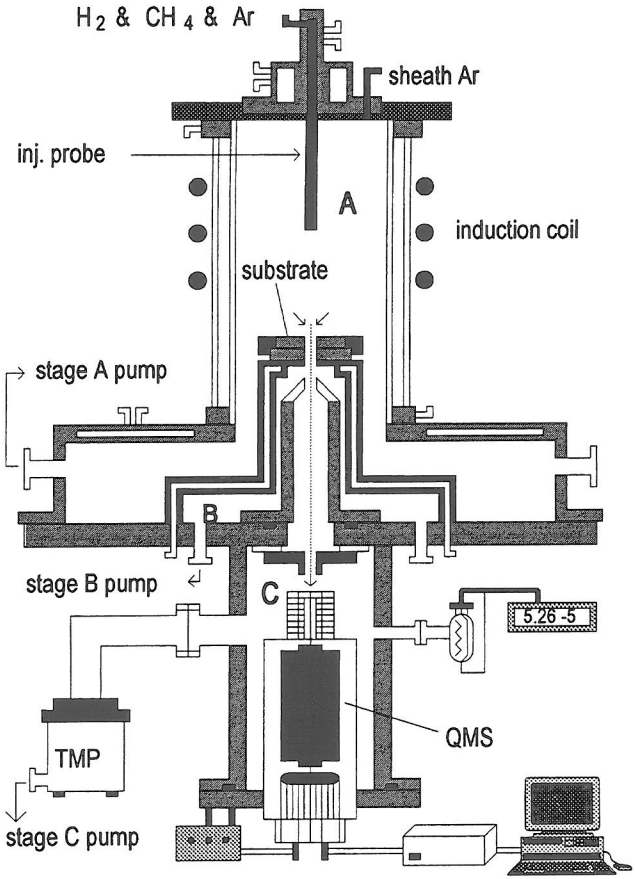

Figure 1. The experimental apparatus.

The differential region (B) is a pressure buffer between the reactor and QMS stages, and has a dedicated pump that maintains a pressure (P_2) below 400 mtorr. The differential stage is enclosed by a cylindrical water-cooled SS shell. At the top of this cylinder a SS supersonic nozzle plate is attached with gold O-rings, allowing for simultaneous water cooling and high vacuum operation. The design of the substrate assembly and expansion nozzle is shown in Fig 2, where subscripts "1" and "2" refer to quantities in the reactor volume and differential region, respectively.

The gas phase composition is sampled from an extraction volume in the boundary layer just above the substrate (Fig. 2). The dimensions of the extraction volume are on the order of the nozzle diameter (300 μm). Assuming continuum flow, the velocity of the expanded gas may be calculated from the cross sectional areas of the

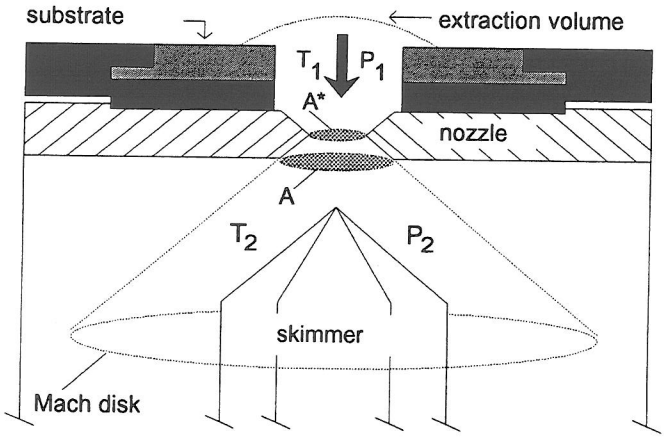

Figure 2. Cross sectional view of the expansion process.

convergent (A^*) and divergent (A) openings in the nozzle, yielding $A^*/A \approx 0.02$ [13]. Using the Mach number (M) and assuming ideal gas behavior, constant γ (C_p/C_v), and isentropic flow within the Mach disk, the temperature drop across the nozzle can be estimated from $T_1/T_2 = 1+(\gamma-1)M^2/2$. For typical operating conditions the Mach number is approximately 4 and the temperature drop (T_1/T_2) is 5, a drop which is sufficient to prevent unimolecular dissociation.

The differential region surrounds a skimmer cone that leads to the high vacuum QMS region (C). The tip of the skimmer is positioned 1-2 mm from the nozzle exit, ensuring that it is within the Mach disk. This is necessary so that sampling occurs within the isentropic region of the expansion, thereby preventing shock waves from interfering with the analysis. Region C contains a quadrupole mass spectrometer (Balzers QMA 420) positioned directly below the skimmer and a turbomolecular pump which maintains a sufficient vacuum for operation of the QMS ($\leq 10^{-5}$ torr) and minimization of the number of bimolecular reactions.

Results

Results for the detection of methyl radicals in a 11.5 kW, 150 torr, $Ar/H_2/CH_4$ (12/1/0.016) discharge are shown in Fig. 3. A threshold ionization technique is used to discriminate methyl radicals present near the substrate surface from methyl fragments produced by ionization of methane within the ionizer of the QMS. The threshold energy for the dissociative ionization of methane, i.e. $CH_4 + e^- \rightarrow CH_3^+ + H + 2e^-$, is 14.3 eV. Therefore, the ionization energy was set at 12.5 eV to ensure that all of the *m/e* 15 signal corresponded to methyl radicals. Figure 3 is a plot of the QMS signal versus the *m/e* ratio. The peak on the left corresponds to CH_3 sampled from the growth region during diamond deposition, and that on the right to CH_4. The relative

sizes of the peaks are not indicative of the relative concentrations of the parent neutrals, because the ionization energy (12.5 eV) is near threshold for the ionization of methane, $CH_4 + e^- \rightarrow CH_4^+ + 2e^-$, and the ionization cross sections for the parent species are quite different at this energy.

In order to quantify the methyl radical concentration, a calibration procedure was used in which the *m/e* 16 signal from methane was obtained for various known methane pressures in the reactor at an ionizer energy of 17 eV. The signal intensity I_{16}, measured at ionizer energy $E_{CH4} = 17$ eV, for a methane mole fraction χ_{16}, was related to the methyl intensity I_{15}, at $E_{CH3} = 12.5$ eV, to determine the methyl mole fraction χ_{15} using Eq. 1.

$$\frac{I_{CH_3}\left(E_{CH_3}\right)}{I_{CH_4}\left(E_{CH_4}\right)} = \alpha \bullet \frac{Q_{CH_3}\left(E_{CH_3}\right)}{Q_{CH_4}\left(E_{CH_4}\right)} \bullet \frac{\chi_{CH_3}}{\chi_{CH_4}} \qquad (1)$$

For these results, the ionization cross section ratio Q_{15}/Q_{16} was found in the literature [14,15] and the term α, which represents a sensitivity factor that takes into account mass discrimination effects associated with gas expansion and QMS efficiency, was assumed to be unity because the CH_4 and CH_3 masses are very close. For the data shown in Fig. 3 the methyl mole fraction was determined to be 2 PPM ± 20%, a reasonable value when compared to simulations which model gas phase composition during diamond growth under similar conditions [1].

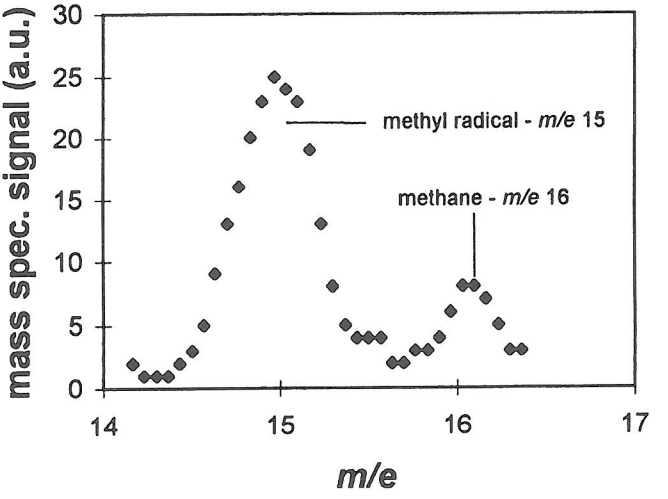

Figure 3. Methyl radical detection using threshold ionization at 12.5 eV.

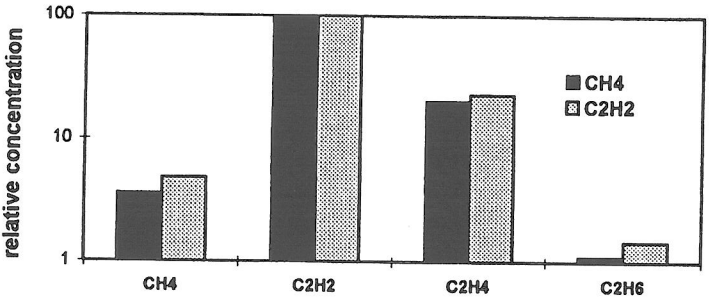

Figure 4. Stable species relative concentrations with CH_4 or C_2H_2 injected.

The relative concentrations of CH_4, C_2H_2, C_2H_4 and C_2H_6 for a 9kW, 220 torr discharge are shown in Fig. 4 as a function of feedstock composition. Both methane ($CH_4/H_2 = 2\%$) and acetylene ($C_2H_2/H_2 = 1\%$) mixtures were studied, with mixture ratios chosen to maintain a similar carbon to hydrogen ratio in the feedstock. The relative concentrations of these species were found to vary only slightly with feedstock composition. For both mixtures, the most abundant species was acetylene, followed by ethene and methane, with little detectable ethane.

Acknowledgment This work is supported by the National Science Foundation through the ERC for Plasma-Aided Manufacturing (CTS-9115464).

References

1. S. L. Girshick *et al.*, Plasma Chem. Plasma Process. **13**, 181 (1993).
2. M. Frenklach and H. Wang, Phys. Rev. B **43**, 1520 (1991).
3. S. J. Harris and D. G. Goodwin, J. Phys. Chem. **97**, 23 (1993).
4. S. J. Harris, Appl. Phys. Lett. **56**, 2298 (1990).
5. T. Mitomo, T. Ohta, E. Kondoh and K. Ohtsuka, J. Appl. Phys. **70**, 4532 (1991).
6. P. W. Pastel and W. J. Varhue, J. Vac. Sci. Technol. A **9**, 1129 (1990).
7. "Experimental Study of Diamond Film Morphology and Surface Chemistry in RF Induction Plasma CVD", Girshick *et al.* to be presented at ISPC 12, 1995.
8. W. L. Hsu, Appl. Phys. Lett. **59**, 1427 (1991).
9. C. E. Johnson, W. A. Weimer and F. M. Cerio, J. Mater. Res. **7**, 1427 (1992).
10. K. Takenchi and T. Yoshida, J. Appl. Phys. **71**, 2636 (1991).
11. W. L. Hsu, M. E. Coltrin and D. S. Dandy, J. Appl. Phys. **76**, 7567 (1994).
12. H. Toyoda, H. Kojima and H. Sugai, Appl. Phys. Lett. **54**(16) 1507 (1989).
13. James D. Anderson, *Modern Compressible Flow: with Historical Perspective* (McGraw-Hill, New York, 1982).
14. D. Wang, L. Lee and S Srivastava, Chem. Phys. Lett. **152**, 513 (1988).
15. H. Chatham, D. Hills and A. Gallagher, J. Chem. Phys. **81**, 1770 (1984).